PROCEEDINGS OF SPIE

SPIEDigitalLibrary.org/conference-proceedings-of-spie

Signal enhancement in microstructured silicon attenuated total reflection elements with quantum cascade laser-based spectroscopy

Jernelv, Ine, Høvik, Jens, Hjelme, Dag Roar, Aksnes, Astrid

Ine L. Jernelv, Jens Høvik, Dag Roar Hjelme, Astrid Aksnes, "Signal enhancement in microstructured silicon attenuated total reflection elements with quantum cascade laser-based spectroscopy," Proc. SPIE 11359, Biomedical Spectroscopy, Microscopy, and Imaging, 113590A (1 April 2020); doi: 10.1117/12.2554528

SPIE.

Event: SPIE Photonics Europe, 2020, Online Only

Signal enhancement in microstructured silicon attenuated total reflection elements with quantum cascade laser-based spectroscopy

Ine L. Jernelv*, Jens Høvik, Dag Roar Hjelme, and Astrid Aksnes

Department of Electronic Systems, Norwegian University of Science and Technology (NTNU), O.S. Bragstads plass 2b, 7491 Trondheim, Norway

ABSTRACT

Sensors in mid-infrared spectroscopy based on attenuated total reflection (ATR) sensing with internal reflection elements (IREs) facilitate easier measurements of aqueous solutions or other opaque analytes. Micromachined silicon (Si) elements are an attractive alternative to conventional IREs, as they can be produced cheaply with silicon processing. Techniques for surface modifications are also easily integrated into the wafer process, and surface structures such as micropillars or nanoparticles can thereby be used for signal enhancement. Replacing the classic Fourier transform infrared (FTIR) spectrometers with tuneable quantum cascade lasers (QCLs) also opens up new avenues for sensing. In this study, the performance of basic and signal-enhanced Si IREs has been compared for measurements in a spectroscopy setup with a fibre-coupled tuneable QCL source. These IREs had V-shaped microgrooves etched on the underside for more efficient in-coupling of light, while the signal-enhanced IREs also had micropillars on the top surface. The results are also contrasted with measurements done in a standard ATR-FTIR spectrometer, using an Alpha II spectrometer with a single-reflection diamond ATR crystal. Various concentrations of glucose (75–5000 mg/dL) in aqueous solutions were used to characterise the system performance. The quality of the signal enhancement was evaluated with regard to sensitivity and noise level in the acquired spectra. The microstructured Si IREs gave a signal enhancement of up to a factor of 3.8 compared to a basic Si element, with some concomitant increase in noise. The absorbance was higher for both types of Si IREs as compared to the diamond ATR crystal. The effective enhancement and the the limit of quantification improved by a factor up to 3.1 in the signal-enhanced IREs compared to the basic Si element.

Keywords: Quantum cascade laser, attenuated total reflection, laser spectroscopy, mid-infrared, glucose

1. INTRODUCTION

Mid-infrared spectroscopy is a routinely used analytical technique, with recent promising developments towards new biomedical applications and miniaturised sensors. Sensors based on attenuated total reflection (ATR) spectroscopy facilitate easier measurements of aqueous solutions or other opaque analytes. Traditionally, relatively large and expensive crystals have been used as internal reflection elements (IREs).[1] Micromachined silicon wafers are an attractive alternative to conventional IREs, as they can be produced cheaply with silicon processing.[2] Additionally, techniques for surface modifications are easily integrated into the wafer process, and surface structures such as micropillars or nanoparticles can thereby be used for signal enhancement. Surface-enhanced infrared absorption spectroscopy (SEIRAS) has been used to achieve enhancement through excitation of localised surface plasmon resonances (LSPRs).[3] LSPRs can be generated at surfaces with rough metal layers or nanoparticles, and are resonant at specific wavelengths depending on the particle sizes. One drawback with this method is that the nanoparticle layer tends to degrade over time, and the substrate has low reproducibility. Another option is to introduce surface modifications through microstructuring, which has been demonstrated on silicon wafer chips.[4–6] Enhancement in different three-layer IRE systems has been demonstrated previously,[7] but the use of silicon is a step forward as it allows for utilisation of semiconductor device manufacturing.

Use of these signal-enhanced IREs enables sensor minaturisation, as they can achieve an increased absorbance signal through evanescent field sensing while maintaining small dimensions. Sensing in reflection mode is an

* ine.jernelv@ntnu.no; phone +47 73594400

Biomedical Spectroscopy, Microscopy, and Imaging, edited by Jürgen Popp, Csilla Gergely, Proc. of SPIE Vol. 11359, 113590A · © 2020 SPIE
CCC code: 0277-786X/20/$21 · doi: 10.1117/12.2554528

advantage for fibre-based applications, and this IRE geometry can potentially be contained on a fibre tip. Conventional silicon IREs are hemispherical, and the larger dimensions limit their use at long wavelengths as silicon has decreased transparency below ∼1400 cm^{-1}. Use of IREs based on silicon wafers makes it possible to measure at longer wavelengths as the typical 500 µm wafer thickness means that optical loss is limited. Replacing classic Fourier transform infrared (FTIR) spectrometers with tuneable quantum cascade lasers (QCLs) also opens up new avenues for sensors. For example, the smaller size of QCLs can contribute to a smaller device footprint. The high spectral power density compared to FTIR spectrometers also means that QCLs can outperform FTIR spectrometers in several applications.

Schumacher et al.[2] demonstrated utilisation of a silicon wafer with V-shaped grooves on the underside in the long wavelength region 1500–300 cm^{-1}. More recently, Sykora et. al.[5] showed that substantial signal enhancement could be achieved by microstructuring the top surface of a wafer. The analytical performance of this microstructured wafer was further studied in an FTIR spectrometer (1800–600 cm^{-1}) by Haas et al.[6] While Haas et al. also showed some spectra from QCL measurements, no results regarding analytical performance were shown. In the present study we quantify the signal enhancement achievable in commercially available microstructured silicon (Si) IREs in a QCL-based spectroscopy setup. The focus of this study is the 1200–925 cm^{-1} spectral range as it is relevant for many biomedical applications, such as glucose sensing.[8] The Si IREs were either basic chips with a flat sensing surface, or surface-enhanced chips with a microstructured sensing surface. The Si IREs were also simulated in order to examine the enhancement effect. A cursory comparison was done with measurements in an ATR-FTIR spectrometer with a diamond IRE.

2. METHODS

2.1 Experimental setup

Measurements in this study were done in a QCL-based ATR spectroscopy setup, see Fig. 1. The experimental equipment for this setup was a QCL source, a photoconductive detector, hollow-core fibres for guiding laser radiation, and internal reflection elements (IREs) for sensing. The laser source was a pulsed external-cavity (EC) QCL (Hedgehog-UT, Daylight Solutions, USA) with a tuning range of 1200–900 cm^{-1} (8.33–11.1 µm). The maximum average output power of the laser was 22 mW with a 5% duty cycle. The laser was cooled thermoelectrically and set to a temperature of 19°C for all measurements. This laser emitted radiation with linear vertical polarisation (100:1, according to specifications). The IR detector was a mercury-cadmium-telluride (MCT) detector (PCI-4TE, Vigo System SA, Poland) with a 2×2 mm element size. The laser beam was focussed into a fibre with an optical assembly mounted on the laser (OKSI fibers, USA). A 300 µm diameter hollow-core fibre (OKSI Fibers, USA) was used to couple light into the IREs, while a 1 mm diameter hollow-core fibre was used to guide light from the IREs to the detector. The laser radiation was found to be elliptical or nearly circularly polarised after transport through the fibres.

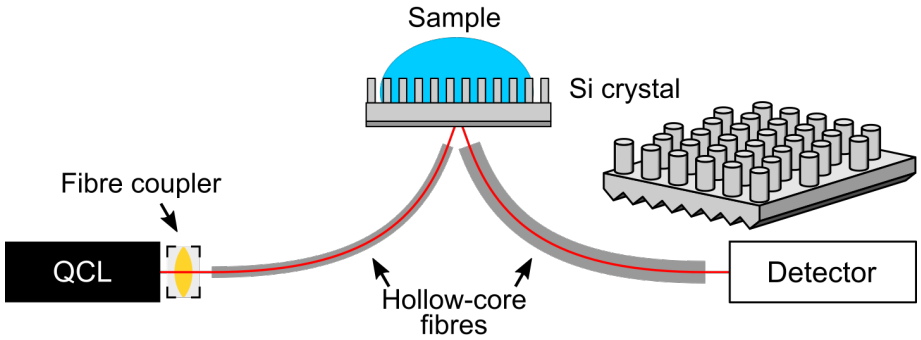

Figure 1: Illustration of experimental setup for the ATR spectroscopy measurements with a QCL source, fibre coupler, hollow-core fibres, Si IRE, and MCT detector. The inset shows a 3D view of an IRE with an optional micropillar enhancement layer. The micropillars are arranged in a hexagonal pattern, and the V-grooves under the wafer are oriented parallel to the laser beam path.

Two types of silicon wafer chips were acquired from IRUBIS GmbH (Germany). These Si IREs had V-shaped grooves etched on the underside for more efficient in-coupling of light. The V-grooves were oriented parallel to the laser beam path. Chips without any further processing had flat top surfaces and were used as standard single-reflection ATR crystals, and will be referred to as "basic" Si IREs. The elements could be further modified on the top surface with a reactive ion etch (RIE) step to create micropillar structures. These micropillar structures facilitate signal enhancement (SE) through an interference effect and field enhancement between the pillars.[9] This effect occurs when the micropillars and the sample form an effective medium layer due to the sub-wavelength sizes of the micropillars. Two IREs with micropillars were investigated for this study, and will be referred to as "SE element #1" and "SE element #2".

Measurements were acquired in an FTIR spectrometer (Alpha II, Bruker Optics Inc., USA) for comparison. This spectrometer was equipped with an ATR module using a single-reflection diamond IRE and had a measurement range of 4000–400 cm^{-1}.

2.2 Data recording

For the QCL setup, measurement spectra were acquired by tuning the laser over a wavelength range and recording the signal on the MCT detector. This analog signal was digitised by an analog-to-digital converter (ADC) card (M2p.5946-x4, Spectrum-Instrumentation GmbH, Germany). The signal was digitised at 80 MS/s with 16 bit resolution. A trigger from the laser controller was used to start data acquisition. The data presented here was recorded in the range 1200–925 cm^{-1}, with a scan speed of 275 cm^{-1}/s.

Averaging, or binning, was used to minimise laser noise. Spectral data points were made by integrating each laser pulse and then averaging a certain number of pulses ($n = 255$ for these measurements). In addition, 10 scans were averaged for each measurement. One spectrum took 10 seconds to record with these settings. Final absorbance spectra were then made by subtracting a background (water) measurement.

For the FTIR measurements, data recording was done with the OPUS software (Bruker Optics Inc., USA). Measurements were recorded in the 4000–400 cm^{-1} spectral range, and 128 scans were averaged for each measurement. The initial spectral resolution was set to 2 cm^{-1}. A zero-filling factor of 2 was used in the OPUS software for the fast Fourier transform (FFT), which gave an interpolation between data points so that the final data point spacing was 1 cm^{-1}. Each measurement in the FTIR spectrometer took approximately 3 minutes.

2.3 Simulations

The Si IREs were simulated in order to investigate the enhancement effect. The simulations were performed using the finite element method (COMSOL Multiphysics v.5.2, COMSOL AB, Stockholm, Sweden.). The simulation geometry was a cross section of the Si IREs in a two-dimensional (2D) environment. The light source was modelled as a plane-wave with an incidence angle of 41° and with in-plane polarisation (i.e. p-polarisation). The boundary conditions between the micropillars and the sample medium relative to the polarisation of the incident light is an important contribution to the increase in field strength. This contribution would disappear if s-polarised light was used, as this periodicity disappears for out-of-plane polarisation in a 2D simulation. The geometry was discretised such that the largest element size was 0.9 μm, roughly 1/10th of the free-space wavelength of the light source. A wavelength sweep was conducted for the wavelength range 1250–893 cm^{-1} (8.2–11 μm) where a surface integration was performed after each simulation to find the total electromagnetic field intensity in the sensing medium (i.e. the medium surrounding the micropillars). Finally the relation between the total field intensity in the sensing area with and without micropillars was calculated to give an indication of the total enhancement of the system.

2.4 Glucose solutions

Measurements were done on glucose solutions, where glucose (D-(+)-glucose, Sigma-Aldrich, USA) was dissolved in demineralised water. A total of 9 samples were made with glucose concentrations in the range 75-5000 mg/dL. A stock solution of 5000 mg glucose in 100 mL water was used to prepare the other samples by dilution.

2.5 Analysis

Calibration curves were made based on the height of the largest glucose absorption band, at approximately 1035 cm^{-1}. The performance of the IREs was then evaluated based on absorbance signal, noise level, limit of quantification (LoQ) and effective enhancement for the signal-enhanced IREs. The enhancement factor was calculated as signal-enhanced/basic absorption peak. Noise was calculated as the RMS-noise of blank spectra in the spectral region 1055–1015 cm^{-1}. Limit of quantification (LoQ) was then estimated based on a signal-to-noise (SNR) ratio of 10:1, where the signal was the height of the most intense absorption band and the RMS noise was the noise level. The effectivity of the signal enhancement was then calculated as the ratio of SNR between the signal-enhanced chips and the basic Si chips.

3. RESULTS AND DISCUSSION

3.1 IRE dimensions

The micropillar structures in the signal-enhanced Si IREs were imaged in a scanning electron microscope (Apreo SEM, FEI Company, USA), see Fig. 2.

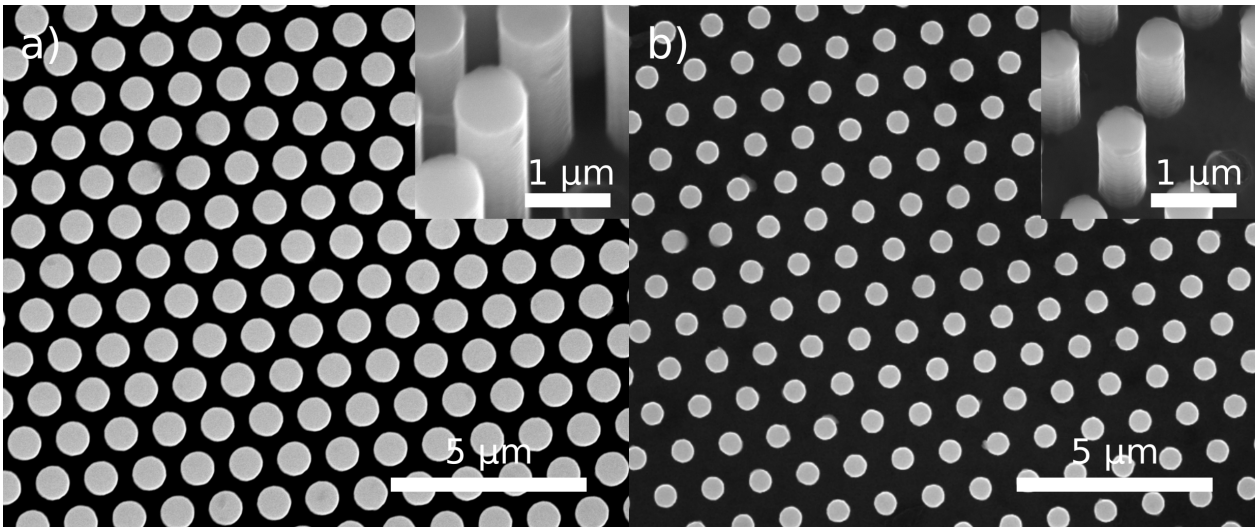

Figure 2: SEM pictographs of Si chips with patterned micropillars, a) SE element #1 and b) SE element #2. The insets show side views at an angle of approximately 25 degrees.

Dimensions of the micropillars are summarised in Table 1. Micropillar dimensions were evaluated with ImageJ, which is an open-source software for scientific image analysis. The pillar periodicity was essentially the same, so the main differences between the IREs were the pillar diameter and height.

Table 1: Geometrical parameters for the Si IREs with micropillar structures.

Dimension	SE element #1	SE element #2
Height	3.5 µm	1.66 µm
Pillar diameter	0.86 µm	0.57 µm
Period	1.25 µm	1.23 µm

3.2 Simulations

Simulations of the field enhancement effect were set up in COMSOL Multiphysics. The flat-topped and the two signal-enhanced elements were all simulated, and the micropillar dimensions from SEM were used for the signal-enhanced elements, see Fig. 3a) for a simulation snapshot.

Enhancement was estimated based on the field intensity in the area above the Si substrate, which was found by a field integration in the sensing medium. The total field intensity in the signal-enhanced IREs was then divided by the field intensity in the basic Si IRE. The resulting enhancement factors are plotted in Fig. 3b) as a function of wavelength. Based on this, SE element #1 had a high enhancement factor that tapered off sharply for wavelengths shorter than 10 µm, while SE element #2 had a more constant enhancement over the available wavelength range.

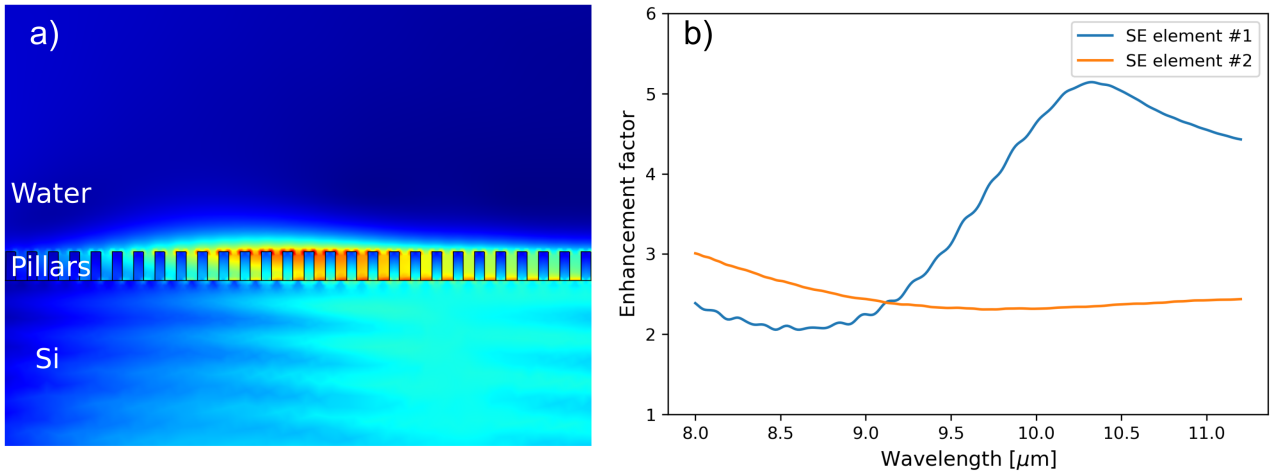

Figure 3: a) 2D structure based on SE element #2 used in the simulations, with evanescent field. b) Enhancement factor in the signal-enhanced Si IREs as a function of wavelength.

These 2D simulations have some limitations with regards to the real micropillar structures. Since the simulations are performed in a 2D environment the model closely resembles a linear array of pillars, even though the IREs themselves utilise a triangular honeycomb lattice. This 2D approximation might therefore lack certain intricacies which might deviate the simulated result from the experimentally verified data. For example, the distance between the pillars will vary between 1.2 µm and 2.1 µm depending on the cross section used for the simulations. We therefore used the pillar radius from SEM, and an average value for the pillar distances. Additionally the light source is not a perfect plane wave but includes field components which are incident on the chip surface with sharper angles than 41°. This leads to some radiation which is caught by the surface integration and thus slightly lowers the calculated amplification of the simulations.

3.3 Comparison between IRE types

Glucose measurements from the FTIR spectrometer with a diamond IRE and the basic Si IRE in the QCL setup are shown in Fig. 4. All glucose absorption bands were found by both methods, but there were some minor structural differences between the measurement sets. For example, the dip at 1000 cm^{-1} was lower for the basic Si element, and the height difference between the absorption bands at 1035 cm^{-1} and 1080 cm^{-1} was larger compared to the diamond IRE. This was likely due to alignment issues in the QCL setup. It was observed that fibre alignment relative to the chip and alignment of in- and out-coupling fibres relative to each other could influence the shape of the absorption spectrum. Overall the absorbance was ~4.5 times higher in the QCL-based setup with an basic Si element compared to the ATR-FTIR spectrometer.

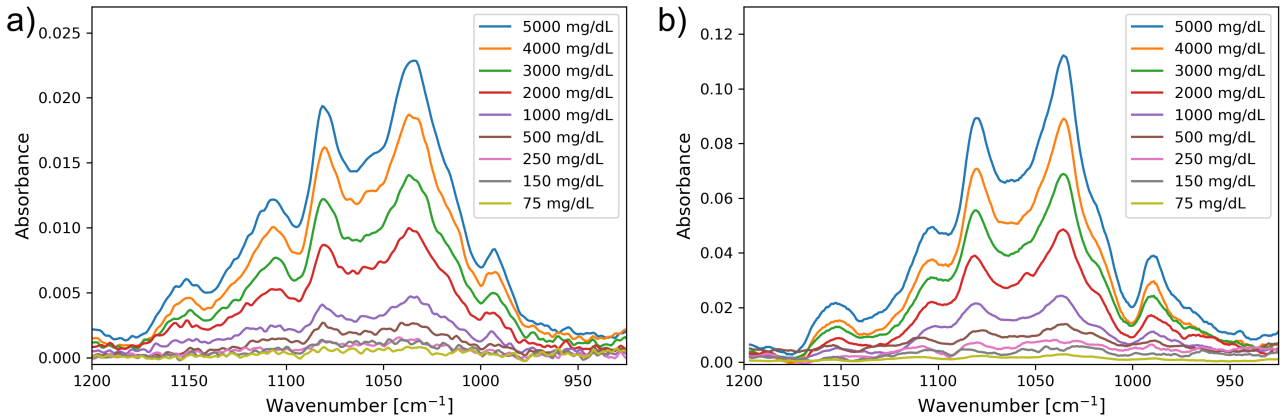

Figure 4: Example spectra from glucose solutions with water background subtracted using a) FTIR spectrometer with a single-reflection diamond IRE, and b) QCL setup with a single-reflection basic Si IRE.

One possible drawback with Si IREs is the formation of a silicon dioxide (SiO_2) layer on the sensing surface, which has been remarked in previous studies.[2,6] Absorption in thick layers of SiO_2 will affect measurements, but thicker layers are mainly formed under high temperature conditions. We expected the layer to be a few nanometers thick, and no clear absorption features could be seen for these IREs.

Measurements from the two signal-enhanced elements are shown in Fig. 5. Both IREs clearly displayed increased absorption compared to the basic Si IRE. The signal in SE element #1 appeared to gradually drop off above approximately 1045 cm^{-1}. This was as expected from the simulations, and the micropillar geometry in this element likely meant that the micropillar layer did not act as an effective medium layer for shorter wavelengths.

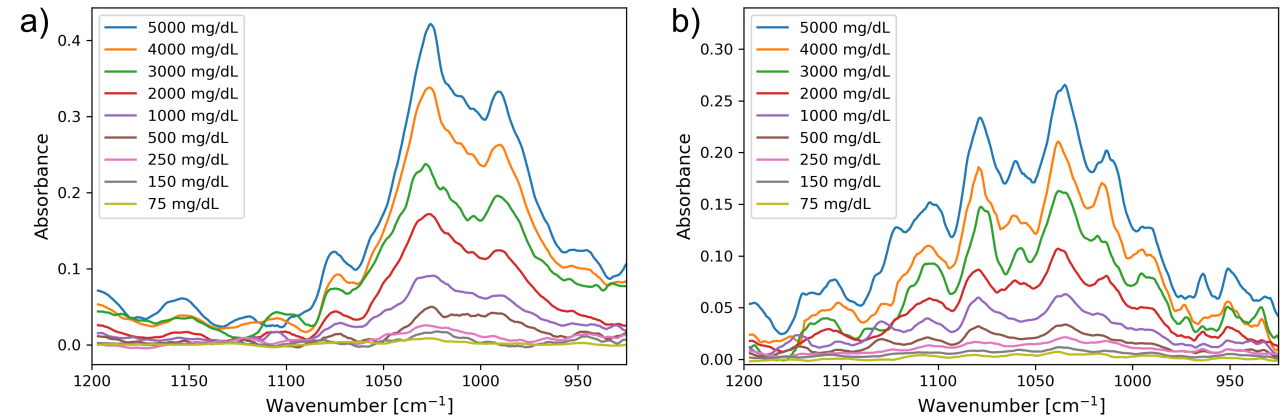

Figure 5: Example spectra from glucose solutions with water background subtracted in the QCL setup using a) SE element #1, and b) SE element #2.

For SE element #2, the signal enhancement was more uniform over the entire wavelength range. However, these spectra had some additional features, such as a splitting of the glucose absorption peak at 1020 cm^{-1}. Fibre alignment was again seen to have a large influence on the appearance of the absorption bands, which was the same behaviour as for the basic Si IRE.

Calibration curves for the measured IREs are shown in Fig. 6. This shows a direct comparison of the highest glucose absorption peaks for the different IREs and setup types. A linear correlation between the absorption peak and the concentration was observed for all IRE types.

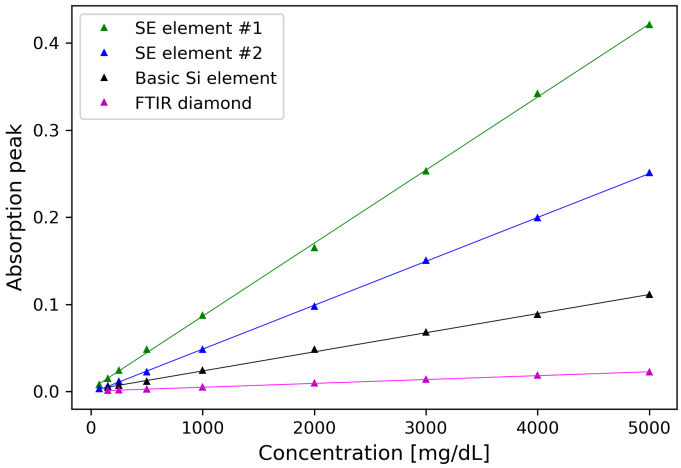

Figure 6: Calibration curves from measurements of glucose concentrations in the four IREs. Signal was measured as the height of the strongest absorption peak, at approximately 1035 cm^{-1}.

The performance of the different IREs is summarised in Table 2. LoQ improved in both signal-enhanced IREs compared to the basic Si IRE. However, the signal enhancement was accompanied by an increase in noise, and the effective enhancement was therefore somewhat lower than what the increase in absorbance signal would indicate. The effective enhancement was a factor of 3.1 and 1.9 in SE element #1 and SE element #2, respectively. The enhancement factors were a bit lower than expected from the COMSOL simulations, but were otherwise consistent. The achieved LoQ of 35 mg/dL indicates that these SE IREs could potentially be used in applications such as glucose sensing, as the range of physiological glucose concentrations in diabetic patients is 30–400 mg/dL.

Table 2: Performance comparison of the basic and signal-enhanced IREs in the QCL-based spectroscopy setup, as well as the diamond IRE in the ATR-FTIR spectrometer. The absorption peak was measured at approx. 1035 cm^{-1} for 5000 mg/dL glucose concentration, and the RMS noise was measured from blank spectra. Effective enhancement in the SE elements was based on the sensitivity improvement compared to the basic Si IRE.

IRE	Absorption peak	RMS noise	LoQ (mg/dL)	Enhancement	Effectivity
SE element #1	0.42	0.00027	35	3.8	3.1
SE element #2	0.25	0.00027	55	2.3	1.9
Basic Si	0.11	0.00022	100	-	-
Diamond (FTIR)	0.023	0.00009	195	-	-

The LoQ was worse in the FTIR spectrometer than the QCL-based setup with even the basic Si IRE, which can be attributed to the lower absorbance signal. The RMS noise was however lower in the spectrometer due to lower relative intensity noise (RIN) in the FTIR source, as well as the longer averaging in the spectrometer. The spectrometer SNR is proportional to $\sqrt{n}$ where n is the number of averaged scans. Noise could therefore have been improved in the FTIR by increasing measurement time and averaging more scans, however the measurement time was already over 3 minutes. This shows some of the advantages that QCLs can have over standard FTIR spectrometers with regards to measurement time and sensitivity.

The main challenges in the QCL-based setup were related to alignment and stability. As mentioned, fibre alignment was seen to influence the shape of absorption bands. However, measurements were repeatable after the setup was stabilised. The noise level was also influenced by vibrations in the fibres, and hence stability was also important for noise minimisation.

4. CONCLUSIONS

This study evaluated the performance of microstructured Si elements with and without a signal enhancement layer as IREs in a QCL-based ATR spectroscopy setup. The signal-enhanced chips were found to improve the absorbance signal up to a factor of 3.8, while due to simultaneous increase in noise the LoQ improved by up to a factor of 3.1. Very different behaviours were seen in the two IREs with micropillars for signal enhancement, which shows that it is important to consider pillar geometry in relation to the wavelength region used. The COMSOL simulations agreed well with the experimental results. 3D simulations should be done in the future to further investigate the effect of the micropillar lattice structure, and the effect of polarisation.

These micromachined Si IREs can be mass-produced and may potentially be integrated in single-use applications for e.g. biomedical measurements. The signal enhancement also gave good LoQs, considering the single-reflection geometries, and another possible application is to use these IREs as sensing surfaces for fibre-optic sensors in reflection mode. This work also demonstrated measurements with Si IREs below 1200 cm^{-1}, which is usually considered opaque for Si components.

ACKNOWLEDGMENTS

The Research Council of Norway is acknowledged for the support to the Norwegian Micro- and Nano-Fabrication Facility, NorFab, grant number 245963/F50, as well as the Double Intraperitoneal Artificial Pancreas project, grant number 248872. The project is part of Center for Digital Life Norway and is also supported by the Research Council of Norway's grant 248810. The authors would like to thank Lorenz Sykora at IRUBIS GmbH for a helpful discussion on the silicon internal reflection elements.

REFERENCES

[1] Jernelv, I. L., Strøm, K., Hjelme, D. R., and Aksnes, A., "Infrared spectroscopy with a fiber-coupled quantum cascade laser for attenuated total reflection measurements towards biomedical applications," *Sensors* **19**(23), 5130 (2019).

[2] Schumacher, H., Künzelmann, U., Vasilev, B., Eichhorn, K. J., and Bartha, J. W., "Applications of microstructured silicon wafers as internal reflection elements in attenuated total reflection Fourier transform infrared spectroscopy," *Applied Spectroscopy* **64**(9), 1022–1027 (2010).

[3] Bibikova, O., Haas, J., López-Lorente, Á. I., Popov, A., Kinnunen, M., Ryabchikov, Y., Kabashin, A., Meglinski, I., and Mizaikoff, B., "Surface enhanced infrared absorption spectroscopy based on gold nanostars and spherical nanoparticles," *Analytica Chimica Acta* **990**, 141–149 (2017).

[4] Morhart, T. A., Unni, B., Lardner, M. J., and Burgess, I. J., "Electrochemical ATR-SEIRAS Using Low-Cost, Micromachined Si Wafers," *Analytical Chemistry* **89**(21), 11818–11824 (2017).

[5] Sykora, L., Müller, A., Kondratiev, A., Roth, A., Mozin, V., Fehr, A., and Zörnack, G., "Silicon ATR crystal with subwavelength structures optimized for blood analysis," *Optical Fibers and Sensors for Medical Diagnostics and Treatment Applications XIX* **10872**, 14 (2019).

[6] Haas, J., Müller, A., Sykora, L., and Mizaikoff, B., "Analytical performance of μ-groove silicon attenuated total reflection waveguides," *Analyst* **144**(10), 3398–3404 (2019).

[7] Huber-Wälchli, P. and Günthard, H. H., "Interference Enhanced Attenuated Total Reflection (IEATR). A new technique for i.r. matrix spectroscopy with high sensitivity," *Spectrochimica Acta Part A: Molecular Spectroscopy* **34**(12), 1253–1262 (1978).

[8] Jernelv, I. L., Milenko, K., Fuglerud, S. S., Hjelme, D. R., Ellingsen, R., and Aksnes, A., "A review of optical methods for continuous glucose monitoring," *Applied Spectroscopy Reviews* **54**(7), 543–572 (2019).

[9] Berz, F., "On a quarter wave light condenser," *British Journal of Applied Physics* **16**(11), 1733–1738 (1965).